Osteoblast and bone tissue response to surface modified zirconia and titanium implant materials

Ralf J. Kohal[1], Maria Bächle[1], Wael Att[1], Saad Chaar[1], Brigitte Altmann[1], Alexander Renz[2] & Frank Butz[1]

[1]Department of Prosthodontics, School of Dentistry, University Hospital Freiburg, Hugstetter Str. 55, 79106 Freiburg, Germany

[2]Fraunhofer Institute for Mechanics of Materials IWM, Woehlerstr. 11, D-79108 Freiburg, Germany

Short Title: Osteoblast/tissue response to implant materials

Correspondence to:
Dr. Frank Butz
Department of Prosthodontics
School of Dentistry
University Hospital Freiburg
Hugstetter Str. 55
79106 Freiburg, Germany
Tel.: +49 761 270 4906
Fax: +49 761 270 4925.
E-mail: frank.butz@uniklinik-freiburg.de

Objective. This study examined the *in vitro* and *in vivo* response of osteoblasts to a novel, acid-etched and sandblasted zirconia surface. *Methods.* Osteoblastic hFOB 1.19 cells were cultured either on electrochemically anodized titanium (TiUnite®), machined titanium (Ti-m), sandblasted and acid-etched zirconia (TZP-proc), and machined zirconia (TZP-A-m). The surface topography of the various substrates was analyzed by 3D laserscan measurements and scanning electron microscopy. At culture days 1, 3, 7, 14, 21, and 28, cell proliferation was determined. Gene expression was analyzed using RT-PCR. Histologic analysis and biomechanical testing was performed on miniature implants placed in the rat femur. *Results.* During the first seven days, a retarded cell proliferation was observed on the TiUnite® surface. After 28 days of cultivation, cell proliferation reached similar levels on all surfaces. An up-regulation of bone and extracellular matrix specific genes could be seen for TZP-proc at day 21. The mean bone-implant contact rate after a healing period of 14 and 28 days, respectively, was higher for TiUnite® than for TZP-proc. At 28 day, the biomechanical test showed significantly higher values for TiUnite® than for all other surfaces. *Conclusions.* The novel, rough zirconia surface was accepted by hFOB 1.19 cells and integrates into rat bone tissue. However, osseointegration seemed to proceed more slowly and to a lesser extent compared to a moderately roughened titanium surface.
(227 words)

Keywords: Dental implants, zirconia, surface topography, histomorphometry, push-in test, cell-culture study, rats

1 Introduction

High bending strength and fracture toughness, resistance to scratching and biocompatibility make zirconia ceramics interesting for dental applications [1]. For patients, zirconia ceramic restorations can mimic the ivory-like appearance of a natural tooth and therefore facilitates improvement of the esthetic outcome [2-4].

More, a noticeably increased number of patients request dental treatments with metal-free reconstructions, with the assumption that desquamation of metal particles and ion release can lead to osteolysis and allergies [5-8]. While titanium has been widely used as implant material for several decades and proved its clinical efficacy [9-13], there is a tendency to design and evaluate zirconia implants due to the above mentioned shortcomings of metals/titanium [14]. At present, the most frequently used material for ceramic oral implants involves yttria-stabilized tetragonal zirconia polycrystal (Y-TZP). The introduction of the hot isostatic postcompaction (HIP) process (= condensation of ceramic particles under high pressure and temperature to obtain a highly dense material) enabled the production of highly compacted zirconia structures with fine grain size and high purity of Y-TZP; improving the material properties and allowing the clinical application as oral implant material (for review see: [15]). Several preclinical studies have shown that oral implants made of Y-TZP may withstand masticatory forces over extended periods [16-19] and animal studies have demonstrated that zirconia implants osseointegrate in a similar manner to titanium implants [20-25].

The success of endosseous oral implants is directly related to the principle of osseointegration, a process of implant-bone interaction that finally leads to bone-to-implant anchorage, which is necessary for long-term success of these implants [26]. The anchorage of implants is typically assessed by several methods like removable

torque [27], pull-out [28] and push-in tests [23, 29]. In this context, implants with rough surfaces are typically associated with higher forces that are required to break the implant anchorage, when compared with smooth-surface implants [27, 29, 30].

Implant surface characteristics including topographical configuration and chemical and physical properties have been demonstrated to influence the initial cell response at the cell-material interface, ultimately affecting the rate and quality of the *de novo* tissue [31-37]. For this reason, investigations concerning cell proliferation and bone-related gene expression are essential to understand cell response to new implant material surfaces. However, surface modification of zirconia is challenging. Sintering particles onto the surface, nano-technology, sandblasting and acid-etching, and laser technology have been used to produce a roughened zirconia surface [38-42].

A novel treatment technology to change the surface properties for zirconia oral implants was recently developed (Patent pending, Patent application number: 20100178636) in order to improve osteoblast cell response and the osseous integration of implants into bone. Therefore, the rationale of this investigation was twofold: 1) evaluation of the behavior of hFOB 1.19 osteoblasts towards the novel zirconia surface and compare it to their behavior on a rough (marketed) titanium surface, a machined titanium surface and a machined zirconia surface; 2) evaluation of the osseous healing (osseointegration) and bone-implant interfacial strength of the novel zirconia surface in a standardized rat femur model.

2 Materials and methods

2.1 Substrate design and surface analysis

Commercially pure titanium and yttria-stabilized tetragonal zirconia polycrystal (Y-TZP) disks (20 mm in diameter and 1.5 mm in thickness) and miniature cylindrical implants (2 mm in length, 1 mm in diameter) were fabricated for this study. The titanium surface was either turned by machining (Ti-m) or roughened by electrochemical anodization (TiUnite®, Nobel Biocare, Gothenburg, Sweden). The zirconia surface was either turned by machining (TZP-A-m) or roughened by sandblasting with Al_2O_3 (grain size 30 to 130 µm) at 4 – 6 bar and acid-etching with hydrofluoric acid, nitric acid, and sulfuric acid with subsequent heat treatment (1200° C. to 1400° C) in order to smoothen the sharp edges as a result of the etching procedure (TZP-proc, Patent pending, Patent application number: 20100178636, VITA Zahnfabrik, Bad Säckingen Germany). All materials were sterilized using low-temperature hydrogen peroxide gas plasma technology (STERRAD 100 / 100S, Advanced Sterilization Products (A.S.P), Johnson & Johnson Medical, Irvine, USA).

The surface of the substrates was examined by scanning electron microscopy (SEM) (Zeiss Leo 32, Zeiss, Oberkochen, Germany) after being gold-palladium-sputtered, and by 3D laser scanning (3D Laser Microscope VK-9700K, Keyence Corp., Osaka, Japan). Average roughness (S_a), the values of peak-to-valley (S_z), average mean spacing of profile peaks in the mean plane as expressed in the x direction (S_{cx}), and the developed surface area ratio (S_{dr}) were calculated.

Raman spectroscopy (inVia Raman Microscope, Renishaw, Gloucestershire, UK) was used to detect the effect of the surface treatment on the Al_2O_3 content and potential tetragonal to monoclinic phase transformations in the zirconia-based ceramic.

2.2 Cell culture

The human osteoblast cell line hFOB 1.19 (ATCC, LGC Promochem, Wesel, Germany) was used for the cell culture experiment. These cells show minimal chromosome abnormalities and synthesize a normal spectrum of matrix proteins [43]. The cells were cultured according to the ATCC recommendations at 33.5°C in a 1:1 mixture of Dulbecco´s Minimal Essential Medium (high glucose) and Hams F12 (Lonza, Verviers, Belgium) with 15 mM Hepes (Biochrom, Berlin, Germany), 0.5 mM Na Pyruvat, 1.2 g/l Na bicarbonate, 0.3 mg/ml G418, 10% fetal calf serum (FCS; Biochrom, Berlin, Germany), 100 U/ml penicillin and 10 mg/ml streptomycin (Biochrom, Berlin, Germany). Cells from passage 5 to 10 were used for all experiments. For cell proliferation h.FOB 1.19 cells were cultured at 33.5°C in a 5% CO_2 humified atmosphere. When cells reached confluence of approximately 80%, they were trypsinated and finally seeded at a density of 1.3×10^4 cells onto the test substrates in 12-well plates. The medium was exchanged every third day for up to seven days. From day 7 until day 28, the medium was exchanged every second day. Since the hFOB 1.19 cell line is immortalized with a temperature-sensitive SV40 large T antigen, which can be inactivated at 39.5°C, cell division is slowly ceased at 39.5 °C and cell differentiation is induced. In our experimental setup cell differentiation was induced in confluent cultures by raising the temperature to 39.5°C.

2.3 Cell proliferation

Cell proliferation was measured with the EZ4U kit (EASY FOR YOU, Biozol diagnostica Corp., Eching, Germany). The assay is based on the mitochondrial reduction of tetrazolium in living cells and the subsequent release of the reduction product formazan into the culture medium. Formazan can be then quantified in the supernatant by spectrophotometrical measurement at 450 nm in a microplate reader. The assay was performed according to the manufacturer's protocol. Cell growth on

polystyrene was used as control. All experiments were performed in triplicate after 1, 3, 7, 14, 21, and 28 days.

2.4 Confocal laser scanning microscopy

Cell surface contact and cytoskeletal arrangement of the osteoblasts on the different substrates were examined by indirect immunofluorescence of the focal adhesion protein vinculin and the cytoskeleton protein actin with a commercial staining kit (Millipore, Billerica, USA). For this purpose, cells were cultured for 1 and 28 days on the different substrates and fixed for 15 min in 4% paraformaldehyde. After fixation, the hFOB 1.19 cells were rinsed with PBS, permeabilized for 5 min with 0.1% TritonX-100 (Sigma Diagnostics, St. Louis, USA) in PBS and incubated overnight with anti-vinculin (mouse anti-human antibody) in a dilution of 1:500. After 24h incubation with the primary antibody, probes were rinsed 3 times with wash buffer (PBS, containing 0.05% Tween-20) and incubated with a FITC-conjugated anti-mouse antibody (green) in a dilution of 1:1000. Actin was detected with TRIC-coupled phalloidin (red) in a dilution of 1:500 after an incubation time of 60 min. The nucleoli of the cells were counterstained with DAPI (blue) for 5 min. Images were acquired using a confocal laser scanning microscope (Leica TCS SP2 AOBS, Leica Microsystems Bensheim, Germany).

2.5 Gene expression analysis

Gene expression of several bone-specific markers (Table 1) was analyzed by semi-quantitative real-time RT-PCR. For this purpose total mRNA from hFOB 1.19 cells was isolated after 3, 7, 14, 21, and 28 days of culture on the different materials using the RNeasy MiniKit (Qiagen, Hilden, Germany). Integrity and concentration of the RNA were determined using a lab on a chip RNA 6000 Nano Series II kit (Agilent Technologies, Waldbronn, Germany) that was run on an Agilent 2100 Bioanalyzer

instrument (Agilent Technologies). Reverse transcription was performed with 5 µg total RNA.

The cells cultured on the discs were harvested by trypsinization and washed with PBS. The primer sequences of selected genes were determined with the “Universal Probe Library” software from Roche (http:qpcr.probefinder.com/organism.jsp). Only intron-spanning sequences were chosen in order to exclude contamination with genomic DNA. Real-time RT-PCR was performed in a Light Cycler 489 (Roche, Basel, Switzerland) in a 384 plate. A 10µl volume with 5µl SYBR Green I Mastermix (Roche), 50 ng cDNA as template and 0.5 µM of the primer-pairs were used respectively.

Light cycling conditions were as follows: activation (95° C for 10 sec.), 40 amplification cycles (95° C for 10 seconds, 52° C for 5 seconds, and 72° C for 12 seconds). Melting curve analysis was used to ensure that all transcripts under investigation were represented by a single peak, indicating specificity. Gene expression was calculated from the real-time RT-PCR efficiency [44] in relation to the mean of five housekeeping genes (LMNA, GAPDH, ACTB, RPS18, and RPLP0). Three independent cultures were used for real-time RT-PCR measurements.

2.6 Placement of experimental implants in the rat femur

Fifty-six 8-week-old male Sprague-Dawley rats were anesthetized with 1% to 2% isoflurane inhalation. After the legs were shaved and disinfected with 0.2% chlorhexidine, the distal parts of the femurs were exposed. One zirconia implant with a sandblasted and acid-etched surface (TZP-proc) and one titanium implant with an electrochemical anodized surface (TiUnite®) were randomly placed into the left and right femurs, respectively, of twenty-eight rats. The remaining twenty-eight rats received one zirconia implant with a turned surface (TZP-A-m) and one titanium implant with a turned surface (Ti-m) which were also randomly placed into left and

right femurs, respectively. The implant site was prepared at 7-9 mm from the distal edge of the femur using a 0.8 mm round burr and reamers (ISO 90). Irrigation with sterile saline solution was used for cooling and cleaning. The implants were installed into the osteotomy and pushed into place until they were even with the femoral bone. The tissues were then closed with resorbable sutures (Vicryl®, Ethicon GmbH, Norderstedt, Germany). Animals with TiUnite® and TZP-proc implants were randomly divided into four groups of seven each. Two groups were killed at week 2 and two groups were killed at week 4 of the healing period. Animals with Ti-m and TZP-A-m implants were also divided into four groups of seven each. Again, two groups were killed at week 2 and two groups were killed at week 4 of the healing period. One of the two groups killed at week 2 and of the two groups killed at week 4 was used for histologic evaluation. The remaining groups were used for the implant push-in test.

The study protocol was approved by the University of Freiburg Animal Research Committee (Study No. G-04/60) and was conducted according to the German Federal Guidelines for Animal Research.

2.7 Histologic procedure and histomorphometric analysis

Bone segments containing the implant were harvested and the specimens were thoroughly rinsed with saline and immersed in 10% buffered formalin for 2 weeks at 4°C. The specimens were then dehydrated in alcohol and finally embedded in photocuring resin (Technovit 7200 VLC, Heraeus Kulzer, Wehrheim, Germany). The non-decalcified embedded specimens were cut using a diamond saw and successively ground to a thickness of approximately 80-100 µm with a grinding system (Exakt Apparatebau, Norderstedt, Germany) [45]. The histologic specimens were then stained with basic fuchsine and examined by light microscopy (Zeiss Axioskop, Zeiss, Oberkochen, Germany).

Histologic examination and computer-assisted histomorphometric analysis were performed at 20x and 40x magnification using a light microscope (Zeiss Axioskop), equipped with a video camera (Color View III, Olympus) and the software program cell* (Olympus). Histomorphometric analysis comprised the evaluation of the fraction of the implant in contact to the mineralized bone tissue over the entire implant length.

2.8 Implant push-in test

A push-in test was performed to assess the biomechanical strength of bone-implant integration [23, 29, 46].

Bone segments containing the implant were harvested, immediately embedded in autopolymerizing resin (Technovit 4071, Heraeus Kulzer, Wehrheim, Germany), and loaded axially in a universal testing machine (Zwick, Ulm, Germany). For the loading a 0.8 mm diameter stainless steel pushing rod was used in a 2000 N load cell and a cross-head speed of 1 mm/min. The applied load and the displacement of the implant were monitored at a sampling rate of 4 Hz. The maximum load prior to a rapid decrease in the load-displacement curve was regarded as the push-in value.

2.9 Statistics

A two-way analysis of variance (ANOVA) followed by one-way ANOVA at $p<0.05$ level of significance was applied to evaluate the effects of substrate types and culture times on cell proliferation and gene expression. Bonferroni multiple comparison was used for *post hoc* testing.

Data of the *in vivo* experiments (histological evaluation and the push-in test) were expressed as mean values $\pm$ standard deviations. For statistical inference, each animal was considered as a cluster because data were collected on two femurs per animal. A repeated measures analysis of variance (ANOVA) has been used to take the within-animal dependence into account. The model assumption, i.e. normal distribution of the residuals, has been checked by looking at the histograms and

normal probability plots. Non-normality could not be detected in the data (Kolmogorov–Smirnov test: P-value > 0.15). The group effects and differences of least-square means were calculated with their 95% confidence intervals. The P-values for the pair wise comparison were adjusted by the Tukey–Kramer method. All calculations have been performed using PROC MIXED and others of the statistical software SAS 9.1.2.

3 Results

3.1 Surface topography of the substrates

The SEM analyses of Ti-m (Fig. 1a) and TZP-A-m (Fig. 1c) exhibited parallel grooves typically resulting from the machining process. TiUnite® (Fig. 1b) showed a different appearance as compared to TZP-proc (Fig. 1d). The microstructured TiUnite® surface displayed smooth areas interspersed with irregular open pores up to 10 µm, while TZP-proc showed an irregular structured surface with rounded uprisings. The three-dimensional surface characterization and surface roughness parameters (Table 2) were obtained by 3D laserscans. The morphology of the surfaces was very different. While the TiUnite® surface had sharp-edged pinnacles (Fig. 1b), TZP-proc exhibited a more flat morphology with smooth hills and valleys (Fig. 1d). Smoother, flat surfaces with grooves from the machining process could be observed on the machined surfaces of Ti-m (Fig. 1a) and TZP-a-m (Fig. 1c). The S_a-values ranged from 1.31 µm for TiUnite® to 0.19 µm for TZP-A-m. No Al_2O_3 was detected on the processed zirconia surface due to acid-etching, but the mechanical surface treatment induced a tetragonal to monoclinic phase transformation (Fig. 2).

3.2 Cellular proliferation

Fig. 3 shows the percentage of formed formazan in cells cultured for 1, 3, 7, 14, 21, and 28 days on the examined surfaces compared to cells on cell culture plastic. The hFOB 1.19 cells on the TiUnite® surfaces proliferated continuously but more slowly in comparison to the other surfaces until day 21. On the TZP-proc surfaces the proliferation increased until day 3 and then the cell quantity remained on a constant level. After 28 days of cultivation, cell proliferation reached the same level on all surfaces.

3.3 Confocal laser scanning microscopy: Evaluation of cytoskeleton development

The cytoskeletal arrangement and morphology of the osteoblasts were examined by indirect immunofluorescence of the focal adhesion protein vinculin and the cytoskeleton protein actin. Osteoblast morphology varied dependent upon which experimental substrate cells were cultured. To visualize the evolution of the cytoskeleton and focal adhesions of hFOB 1.19 after culturing 1 and 28 days on the different surfaces, actin and vinculin immunostaining was used (Fig. 4). Regarding cell-adhesion on the surfaces after 1 day it could be observed that on PE control nearly all cells had contact to each other (actin, red) and have established a distinct cytoskeleton. The nucleoli of the cells appeared blue by immunostaining with DAPI. The integrins (vinculin, localized within the adhesion complex) are green labeled and at day 1 less pronounced on TiUnite® and TZP-proc compared to Ti-m and TZP-A-m. Furthermore, the distribution of vinculin was more homogenous on the smooth surfaces Ti-M, TZP-A-m, and PE. On TiUnite® and TZP-proc surfaces, there were cells with an intense green staining and cells were no vinculin could be detected. The expression of the cytoskeleton on the modified surfaces was less intense and on TiUnite® not developed at day 1. On the TiUnite® surface, many rounded cells could be seen whereas on the other surfaces, the cells presented with extensions and filopodiae looking for intercellular contact. However, the intensity of the actin filaments was similar on all surfaces.

At day 28 of the cell culture, a pronounced cytoskeleton was found in all groups. However, the actin staining was less pronounced on TiUnite® surfaces than on all other surfaces.

3.4 Gene expression analysis: Real-time RT-PCR

The differences in gene expression on the different surfaces were examined in comparison to cells cultured on polystyrene (PE) and the results are shown in Fig. 5 a-d and Fig. 6a-d. RUNX3 is a member of the RUNX family transcription factors [47] and was detected in osteoblasts throughout the entire cell cycle, especially during proliferation and later in the mineralization phase of the cells [48]. This factor is upregulated on all surfaces but more pronounced on Ti-m at day 3 (p=0.075) and on the TZP-proc surface at day 21 (p=0.0001) (Fig. 5a).

BMP7 plays a key role in the transformation of mesenchymal cells into bone and cartilage producing cells. On TiUnite® BMP7 was significantly more upregulated at day 3 compared to the zirconia surfaces (p=0.002). There was a noticeable upregulation on the TZP-proc surface and a downregulation on the titanium surfaces at day 21 (p=0.0001) (Fig. 5b).

COL1A1 and COL2A1 genes encoding for osteoblast matrix proteins seemed to be only little regulated except for day 21 when a significant upregulation occurred on the TZP-proc surface (both: p<0.0001) (Fig. 5c-d).

IBSP (Fig. 6a) is expressed to bind to other integrins available in the matrix. Integrins are required for extracellular matrix (ECM) adhesion and migration. They are involved in matrix maturation and mineralization. IBSP was not upregulated until day 21. The upregulation of IBSP was significant on the TZP-proc substrate (p<0.0001). TZP-proc also induced a significant upregulation of ITGB1 (p<0.0001) (Fig. 6b).

Biglycan (BGN) belongs to the proteoglycans which play a role in the attachment and adhesion between osteoblastic cells and the ECM [49, 50]. BGN is an essential component of the ECM and was upregulated at day 21 and significantly more on the TZP-proc surface compared to all other surfaces (p<0.0001) (Fig. 6c). At day 28,

BGN was downregulated on TZP-proc whereas the BGN on the other surfaces remained almost on the level of day 21 (p=0.007).

Osteocalcin (BGLAP) is a bone specific marker for matrix mineralization and ECM maturation and binds calcium in the bone matrix. TZP-proc induced a specific and pronounced up-regulation of BGLAP at day 21 (p<0.0001). At day 28, this gene remained only upregulated on TiUnite® and a significant downregulation was seen on the TZP-proc surface (p<0.0001) (Fig. 6d).

3.5 Animal experiment: Clinical and histological observations

All animals recovered well from the surgical intervention. Healing after surgery was uneventful for all animals. No signs of infection or adverse tissue reactions at the site of implantation were observed.

During the preparation of the histological specimens five implants in total were lost. One implant in the 14 day Ti-m group, two implants in the 28 day Ti-m group, one implant each in the 28 day TiUnite® group and the 28 day TZP-proc group.

The histological evaluation showed direct mineralized bone contact to all zirconia and titanium surfaces interspersed with bone marrow-to-implant contact. Newly formed bone trabeculae in direct contact with the implant surfaces could be observed in all four groups at 14 and 28 days (Fig. 7). The bone-to-implant contact increased over time for all groups (Table 3). The mean mineralized bone-to-implant contact after 14 days of healing amounted to 23% for Ti-m, 31% for TZP-A-m, 36% for the TiUnite® group and 18% for the TZP-proc group. The bone-to-implant contact was significantly lower in the TZP-proc group compared to TiUnite® (ANOVA: p<0.0084). After 28 days, the bone-to-implant contact increased in all four groups: Ti-m = 39%, TZP-A-m = 47%, TiUnite® = 56%, TZP-proc = 34%. At 28 days no statistically significant difference could be found between any of the groups (ANOVA: p=0.1719).

3.6 Animal investigation: Implant push-in test

The push-in tests were performed at 14 and 28 days after healing with a universal testing machine and the stainless-steel pushing rod. The push-in values at 14 days were 19 N for Ti-m, 19 N for TZP-A-m, 27 N for TiUnite®, and 26 N for TZP-proc (Table 4). The differences were not statistically significant. The push-in values dropped from 14 to 28 days in the machined groups (Ti-m: 7 N, TZP-A-m: 9 N) but increased for TiUnite® (49 N) and TZP-proc (31 N). There were statistically significant differences between the TiUnite® group and all other groups as well as between the TZP-proc group and the machined groups (Table 4).

4 Discussion

The present investigation as a series of *in vitro* and *in vivo* experiments aimed to evaluate osteoblast and bone tissue responses to a commonly used titanium implant material and a zirconia implant material with a novel surface modification. The investigation revealed the following findings: (a) osteoblast behavior on the novel zirconia surface was similar to the machined surfaces (cell proliferation) and on the other side similar to the rough titanium surface (cytoskeleton). Regarding the gene expression analysis the modified zirconia surface has a unique position, since at day 21 all evaluated genes were significantly upregulated on this surface; (b) the modified zirconia surface performed not as good as all the other surfaces and materials regarding osseointegration in the animal investigation.

Periimplant osteogenesis is known to be a multistep process including osteoblast adhesion to the surface of a material, proliferation and differentiation, involving the production of specific proteins and the deposition of calcium phosphate in the extracellular matrix [51]. The cell-biomaterial interaction and the attraction of bone-forming cells is a determinant factor for this interface, as it is one of the first steps to occur shortly after implant placement [52]. The kinetics and the extent of osteoblastic cell adhesion to biomaterials are known to depend functionally on the nature of the substrate [32]. So, *in vitro* characterization of cell behavior and compatibility, cell morphology and growth encompasses many essential biological processes [53]. Addressing proliferation, the (“rough”) TiUnite® surface induced a slower proliferation of cells compared to the other (“smooth”) substrates. Up to day 7, the cells on this substrate seem to have to bridge “pores” which are surrounded by flat areas. Later, when this surface-roughness (S_a: 1,31 µm) is partially covered by cells and extracellular matrix (ECM), it may be easier for cells to attach and then proliferate. The reduced proliferation on rough surfaces was also described by other authors [37,

52, 54, 55] and in a former study of our group [56]. In contrast, the TZP-proc surface was showing rather characteristics of a quite smooth surface (S_a: 0.95 µm) where the cells had not to overcome such unevenness. The relatively smooth character of this surface was also shown in the 3D laserscan figure. After 28 days of cultivation, the cell proliferation is similar on all surfaces since the surfaces were covered by cells and uneven areas were evened out through cell layers.

Osteoblasts are adherent and anchorage-dependent cells and have to attach to extracellular matrix (ECM) proteins, such as fibronectin, to function and differentiate properly [57]. This attachment is mediated by specific structures, namely, focal adhesions (FAs), which function as anchoring protein complexes between the actin cytoskeleton of the cells and ECM [58]. The assembly of FAs in response to adhesion to the ECM is gradual, usually occurring within 1 to 2 h after cell attachment. FAs serve at least two significant cellular functions: to transmit force or tension at adhesion sites to maintain strong attachments to the underlying ECM and to act as signaling centers from which numerous intracellular pathways emanate to regulate cell growth, survival and gene expression [59, 60]. The focal adhesion spots are the attachment sides which fix the cells also to an artificial surface. This cell surface contact was visualized by the focal adhesion protein vinculin together with the cytoskeleton protein actin (ECM) [56]. Using morphometric analysis, it appeared that on the surfaces of Ti-m, the TZP-proc and the TZP-A-m cell morphologies and focal adhesions were similar after 1 day of culturing. Only the PE surface had more flattened cells covering a greater surface area with a pronounced network of actin filaments. The osteoblastic cells on the TiUnite® surface expressed less focal adhesion spots and less spreading because they had to bridge – as mentioned above - the unevenness of the surface (“hills and valleys”) slowly. At day 28, the actin filaments were developed to a minor extent in the cells on TiUnite® compared to the

other substrates. This again may confirm that hFOB 1.19 cells identified TiUnite® as rough and TZP-proc more likely as a smooth surface as Ti-m, TZP-A-m and the PE control. On the smooth surfaces, the cells showed greater focal contact formations which correlated directly to the degree of cytoskeletal organization on the respective surface. Based on our observations regarding the focal adhesion protein vinculin, it appears that on all examined surfaces cells were able to adapt to the irregular terrain of the substrate, thereby maximizing cell-surface contact and stabilizing the cytoskeleton.

To further investigate the interaction of prospective implant materials with osteoblast cells, we examined the gene expression profiles of the hFOB 1.19 cells on the different substrates. The modulated expression of selected bone and extracellular matrix related genes may reflect the biologic effect of implant topography and give more detailed information at the molecular level. The gene expression of RUNX3, BMP7, COL1A1 and COL2A1 in the early proliferation stage on day three of cell culture was therefore evaluated. In addition, genes important for the mineralization of the extracellular matrix (IBSP, ITGB1, BGN, BGLAP) were also examined.

The osteoinductive transcription factor RUNX3 was up-regulated at day 3 on Ti-m (however, the upregulation did not lead to significant differences) and at day 21 on TZP-proc. Although this transcription factor plays an important role in switching on or off the expression of different genes, it seemed that the influence of the different surfaces in our investigation on this gene seemed to be negligible.

A significant upregulation of BMP7 occurred at day 3 on TiUnite® and at day 21 on TZP-proc giving the impression that the modified surfaces exert a certain influence on this gene. Such an upregulation was also found in a former study of our group at day 3 for the TiUnite® surface [56]. The bone ECM-related genes COL1A1 and COL2A1 - which are suggested to be osteoblast differentiation markers - as well as

the genes for IBSP, ITGB1, BGN, and BGLAP were upregulated at day 21 especially in the TZP-proc group.

These results are in general in accordance to results of other authors having performed similar investigations [56, 61]. The upregulation of IBSP implied that cells started to build their ECM. The effects of ECM proteins on the growth of bone cells are mediated mainly via integrin receptors. Integrins form a part of the FAs which are primarily responsible for cell attachment and spreading by physically linking integrins to actin cytoskeleton [62]. Also genes that play a role in extracellular matrix maturation (BGLAP) and mineralization (BGN) were upregulated. Osteocalcin (BGLAP) a typical marker of bone development is expressed at a point of time where calcium is stored into ECM. TZP-proc and, to a lesser extent, TiUnite® seemed to support this cellular process in our experiment especially at day 21.

In our investigation, it was observed that most of the examined genes were noticeably upregulated at day 21 and here especially on the TZP-proc surface. This may imply the importance of this timepoint (BMP7 was also upregulated at day 3) for differentiation and matrix maturation, and finally in bone formation and osseointegration of implant materials. However, the reason and the effect of the upregulation of the different genes on the TZP-proc surfaces especially are not clear. Furthermore, the precise interaction between the discussed genes and their impact on bone formation could not be answered with our cell investigation. The matter of interest was therefore whether there is a difference in the osseointegrative capacity of the TZP-proc surface compared to the other surfaces due to the increased upregulation of genes at day 21. An *in vivo* investigation where the direct interaction between bone and implant material can be tested was therefore initiated after the cell culture investigation.

The rat femur bone was chosen as animal model for studying the biological mechanisms of the osseointegration process at two different stages of bone healing around titanium and zirconia implants. It offers a valid model of describing bone-implant interactions and has been used to study the bone-to-implant interface [63-65]. Furthermore this model has been used to examine surface topography effects on the extent of osseointegration [66].

The surface topography, chemistry, and roughness influence the rate and quality of new tissue formation around an implant [67]. Modification of implant surface roughness increased the mechanical fixation of implants [29, 30, 68-70], and therefore the biomechanical strength evaluation at the implant-bone interface is an important assessment parameter for osseointegration [71]. Ogawa et al. [29] established the biomechanical push-in test which we have also used in our experiment as a model for osseointegration research. They have shown that there is a variation in push-in values depending on the surface topography and healing time. The push-in value of an acid-etched and modified titanium implant surface was 3x that of a machined implant after 14 and 28 days. In the present animal investigation, the modified TZP-proc surface showed a lower roughness than the modified titanium surface TiUnite® (S_a/S_z: 1,31/12,38 µm for TiUnite and 0.95/7,93 µm for TZP-proc) and a similar roughness like the machined surfaces. The osseointegrative capacity (bone-to-implant contact) of the novel zirconia surface was the lowest of all tested surfaces after 14 and 28 days of healing (although the results were not statistically significant at 28 days). This fact indicated that the modifying procedure (TZP-proc) did not improve the osseointegrative capacity of the zirconia material when compared to the machined zirconia (TZP-A-m). For the healing bone tissue, the TZP-proc surface had the features of a smooth surface and therefore the bone-to-implant contact was inferior compared to the modified titanium surface and not different when

compared to the machined surfaces. On the other hand, the push-in values after 14 days of healing were similar for the TZP-proc and the TiUnite® surfaces. After 28 days of healing, the push-in values increased for TZP-proc and TiUnite®. This, obviously contradictory, development for the TZP-proc surface could possibly be explained with the intermediate roughness of this surface. The surface seemed to be too smooth to improve osseointegration. However, it might have been rough enough for bone cells to deposit mineralized bone into the undercuts of the surface and therefore to increase the interfacial shear strength. Furthermore, the roughness of the TZP-proc surfaces might have still been able to lead to an improved bone quality as described by Butz et al. [30]. Those authors reported on harder and stiffer bone when rough surfaces were applied and that „the intrinsic biomechanical properties of peri-implant bone can be enhanced by an acid-etched titanium implant surface, providing novel evidence that supports the dominance of anchorage of roughened implants over those with a relatively smooth, machined surface“.

Bone healing is a combination of events of bone formation and remodeling of surrounding tissues [72, 73]. Surface modifications can enhance bone healing and integration of implants and result in higher bone-to-implant contact ratios [27, 68, 69, 74]. Our investigation supports the findings that the surface modification for the titanium but not for the zirconia implants resulted in higher bone-to-implant contact compared with the machined surfaces. We believe that a new implant surface (on a new implant material) should present at least the same positive results in respect to tissue response as modern, accepted implant surfaces provides at the moment.

Other animal investigations, evaluating zirconia implants, could show that modifications of zirconia surfaces led to improvements in the bone-to-implant contact. The results obtained with modified zirconia implant surfaces were comparable to rough titanium surfaces [23-25, 41, 75, 76].

Our investigation is unable to reveal links or relations of the different biological processes of osteoblast behavior and the *in vivo* osseointegration. The osteoblast bioactivity results in the cell culture have shown that the TZP-proc surface was probably recognized by the cells as a surface between the machined titanium and zirconia surfaces and the rough titanium surface. However, a unique feature of the TZP-proc surface was the upregulation of different genes at day 21. The results from the cell cultures were encouraging but these were not entirely reflected in the *in vivo* investigation. Further investigations have to determine whether a modification of the surface treatment will affect the subsequent biological events and eventually the level of osseointegration.

5 Conclusions

Our study showed that the zirconia materials were biocompatible and the cell response was comparable to titanium which still presents the implant material of choice for oral implant fabrication. Whether there is a correlation between the up-regulation of the different genes on the modified zirconia surface (TZP-proc) at day 21 and the reduced bone-to-implant contact especially at day 14, needs further investigation.

In the *in vivo* experiment, TZP-proc performed worse than a standard titanium implant surface modification. Therefore, the modified zirconia surface TZP-proc has to be reassessed after the topography was changed towards a moderately rough surface.

Due to the results of the present investigation, changes in the surface processing will be performed by the producing company and the successor surface is under evaluation at the moment.

6 Acknowledgments

The investigations were supported by a grant of VITA Zahnfabrik Vita, Bad Säckingen, Germany (Contract number FKS360-20061215). The titanium materials were kindly provided by Nobel Biocare, Gothenburg, Sweden.

7 Tables

Table 1. Forward, reverse primers and probe sequences for gene expression analysis

Gene transcript	Code	Forward	Backward
Housekeeping genes			
GAPDH	NM_002046.3	agccacatcgctcagacac	Gcccaatacgaccaaatcc
RPLP0 (Ribosome large SU)	NM_001002.3	ctggaaaacaacccagctct	gaggtcctccttggtgaaca
LMNA	NM_170707.2	ctggtcacccgctcctac	acatgatgctgcagttctgg
ACTB	NM_001101.3	attggcaatgagcggttc	ggatgccacaggactccat
RPS18 (Ribosome small SU)	NM_022551.2	tgcgagtactcaacaccaaca	gcatatcttcggcccaca
Proliferation			
BMP7 (OP-1)	NM_001719.1	tcagcgtttatcaggtgctc	ccagagggtacggctgtc
IBSP (Integrin binding sialoprotein)	NM_004967.3	actgccagaggctcactcc	tcattttggtgattgcttcct
COL1A1 (Typ I Collagen)	NM_000088	caagagtggtgatcgtggtg	gcctgtctcacccttgtca
COL2A1 (Typ II Collagen)	NM_001844	agagggcaatagcaggttca	gcgtgaggtcttctgtgacc
Extracellular matrix maturation			
BGLAP (Osteocalcin)	NM_199173.2	tgagagccctcacactcctc	acctttgctggactctgcac
ITGB1 (Integrin beta 1)	NM_012278.1	tccaaagtcagcagagacctt	atttccagggcttgggata
Mineralization			
RUNX3	NM_001031680	tcagcaccacaagccactt	aatgggttcagttccgaggt
BGN (Biglycan)	NM_001711	cagcccgccaactagtca	ggccagcagagacacgag

Table 2. Surface roughness measured with 3D lasercanner (n=3)

	S_a (µm) (SD)	**S_z (µm) (SD)**	**S_{cx} (µm) (SD)**	**S_{dr} (%) (SD)**
Ti-m	0,58 (0,09)	4,78 (0,7)	1,12 (0,11)	12,3 (0,07)
TiUnite®	1,31 (0,17)	12,38 (0,7)	1,13 (0,04)	29,6 (0,23)
TZP-A-m	0,19 (0,02)	2,48 (0,3)	1,01 (0,02)	11,5 (0,04)
TZP-proc	0,95 (0,41)	7,93 (1,81)	0,99 (0,01)	21,2 (0,06)

S_a = Arithmetic mean of the absolute values of the surface point departures from the mean plane.
S_z = Average value in micrometres of the absolute departures of the five highest peaks and the five deepest valleys
S_{cx} = Average mean spacing of profile peaks in the mean plane, expressed in the x direction.
S_{dr} = Developed surface area ratio, the ratio of the developed surface area to the projected sampling area.

Table 3. Average bone-to-implant contact values (BIC) of the examined surfaces (n=7)

	BIC (%) (SD)	
	Day 14	Day 28
TiUnite®	36.2 (12.9)^{A}	56.1 (15.8)^{A}
Ti-m	23.2 (6.3)^{A,B}	39.4 (3.9)^{A}
TZP-proc	17.6 (1.4)^{B}	33.5 (4.1)^{A}
TZP-A-m	30.9 (10.1)^{A,B}	46.6 (13.89^{A}
	p=0.0084	*p*=0.1719

Same superscript letter not significantly different (ANOVA). SD, standard deviation.

Table 4. Average push-in values of the examined surfaces (n=7)

	Push-In Test Value (N) (SD)	
	Day 14	Day 28
TiUnite	26.5 (15.4)^{A}	49.0 (8.9)^{B}
Ti-m	18.8 (10.6)^{A}	7.3 4.49^{A}
TZP-proc	25.8 (13.8)^{A}	30.6 (9.6)^{C}
TZP-A-m	18.9 (11.8)^{A}	9.3 (4.8)^{A}
	p=0.5483	p<0.0001

Same superscript letter not significantly different (ANOVA). SD, standard deviation.

8 Figures

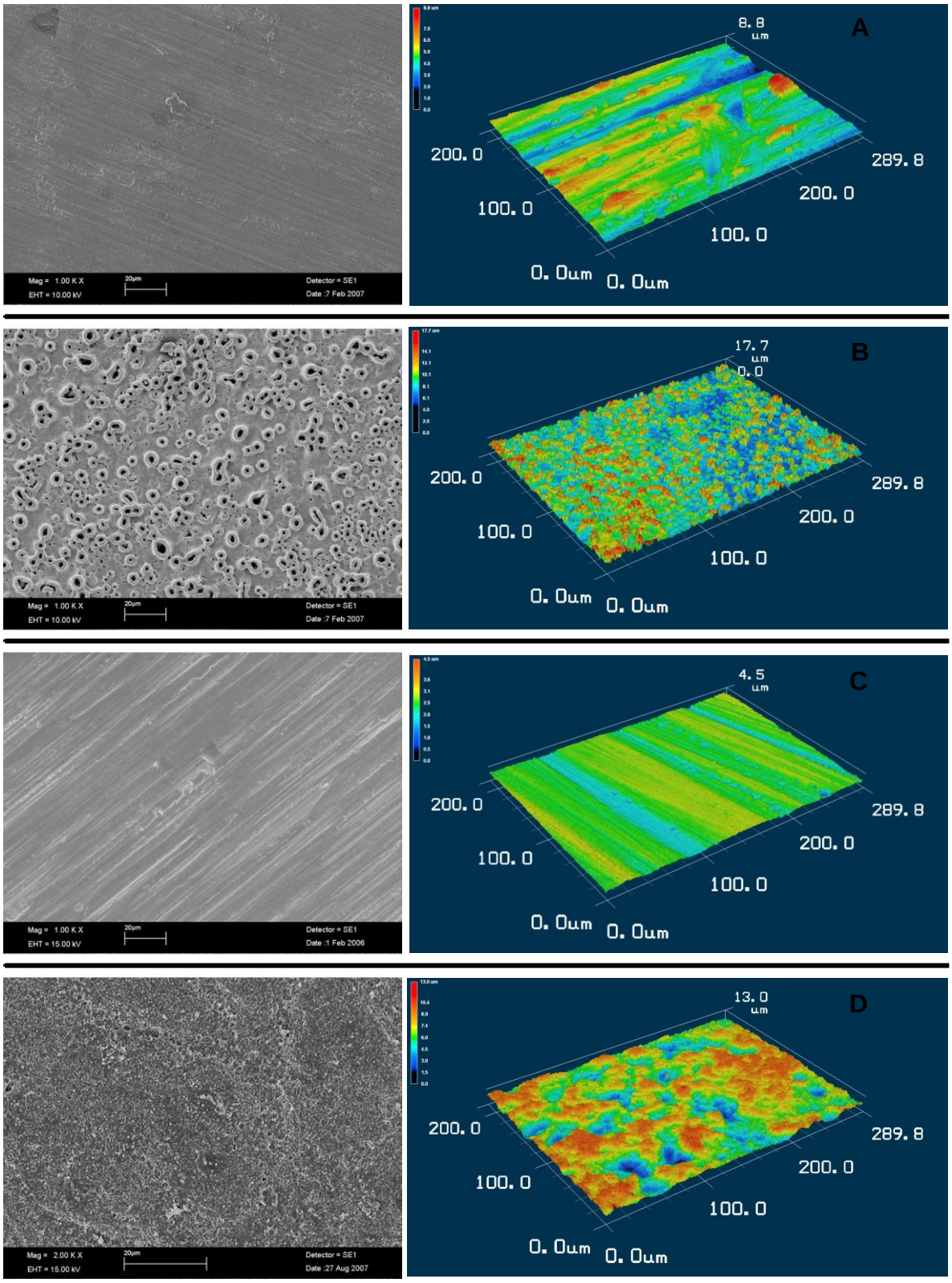

Fig. 1. SEM and correspondent 3D laserscan images of the examined surfaces: Ti-m (A), TiUnite® (B), TZP-A-m (C), TZP-proc (C).

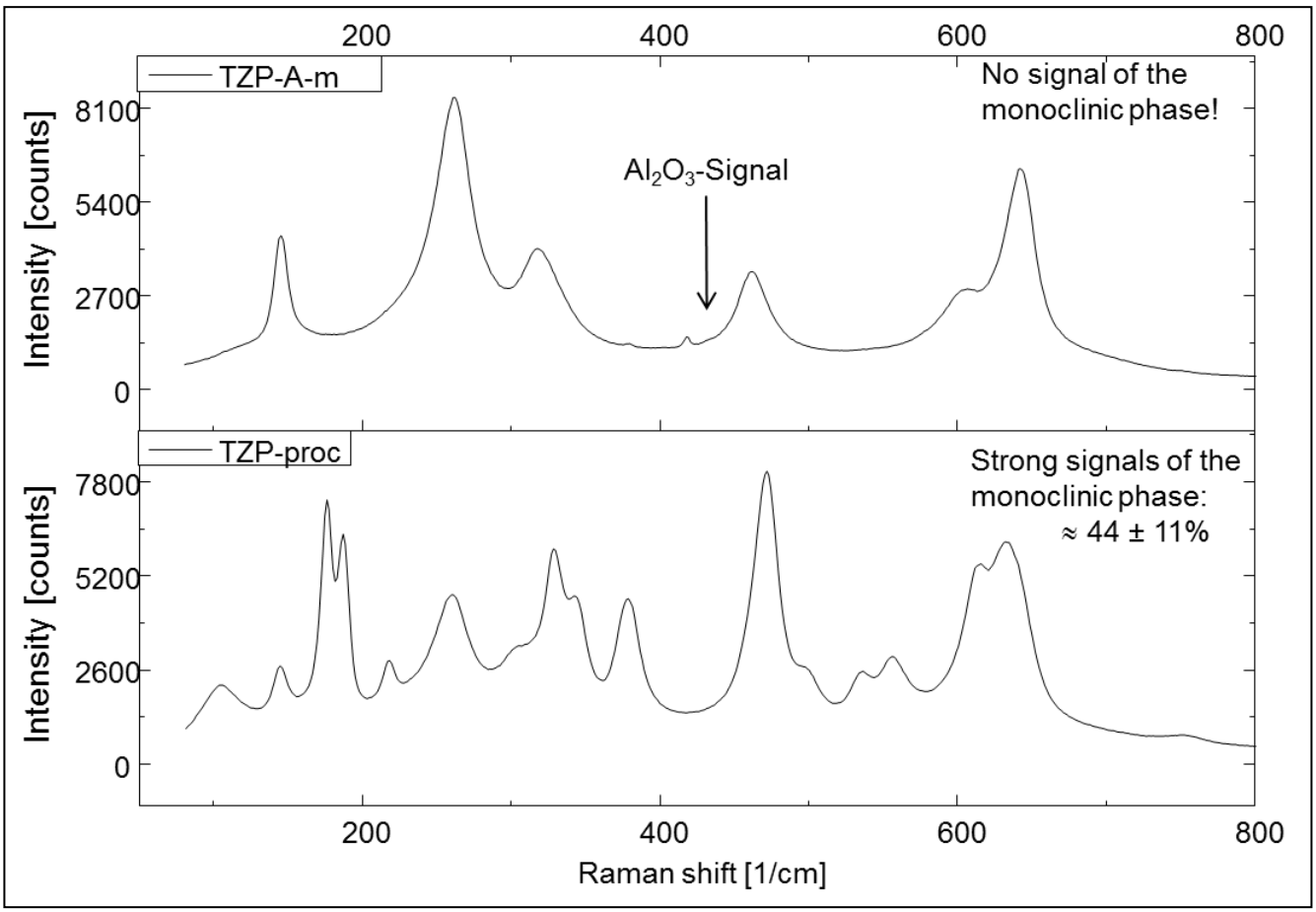

Fig 2. Raman spectroscopy. No Al_2O_3 was detected on the processed zirconia surface (TZP-proc). The mechanical surface treatment induced a tetragonal to monoclinic phase transformation.

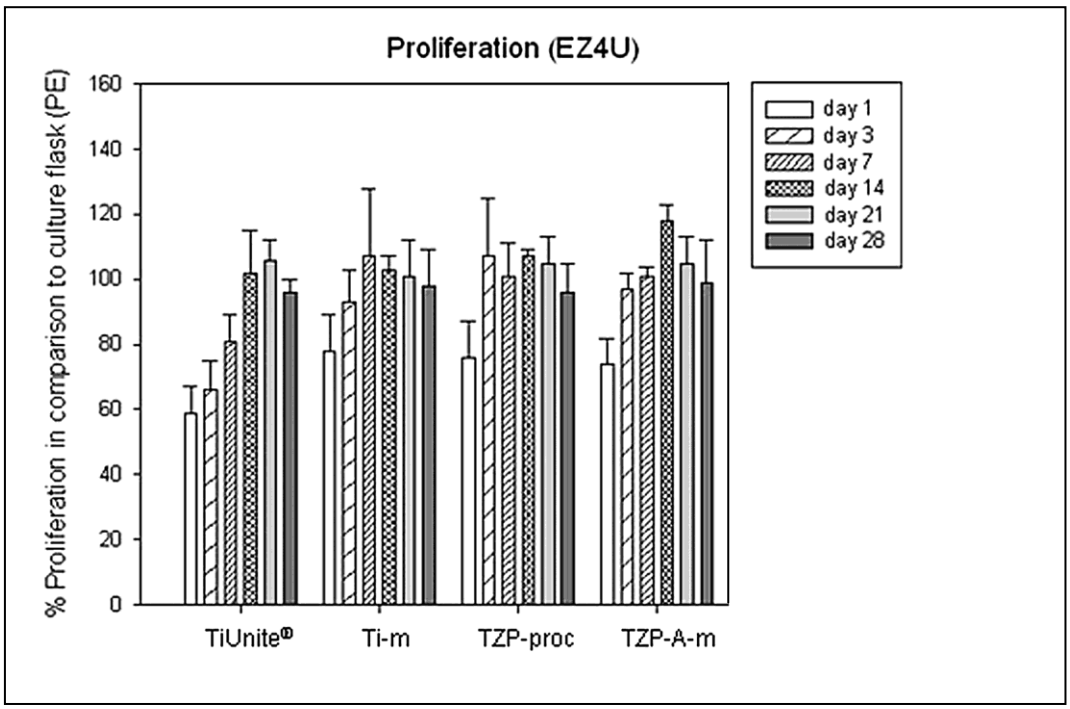

Fig. 3. Percentage of formed formazan in cells cultured for the different time periods on the examined surfaces compared to cells on cell culture plastic.

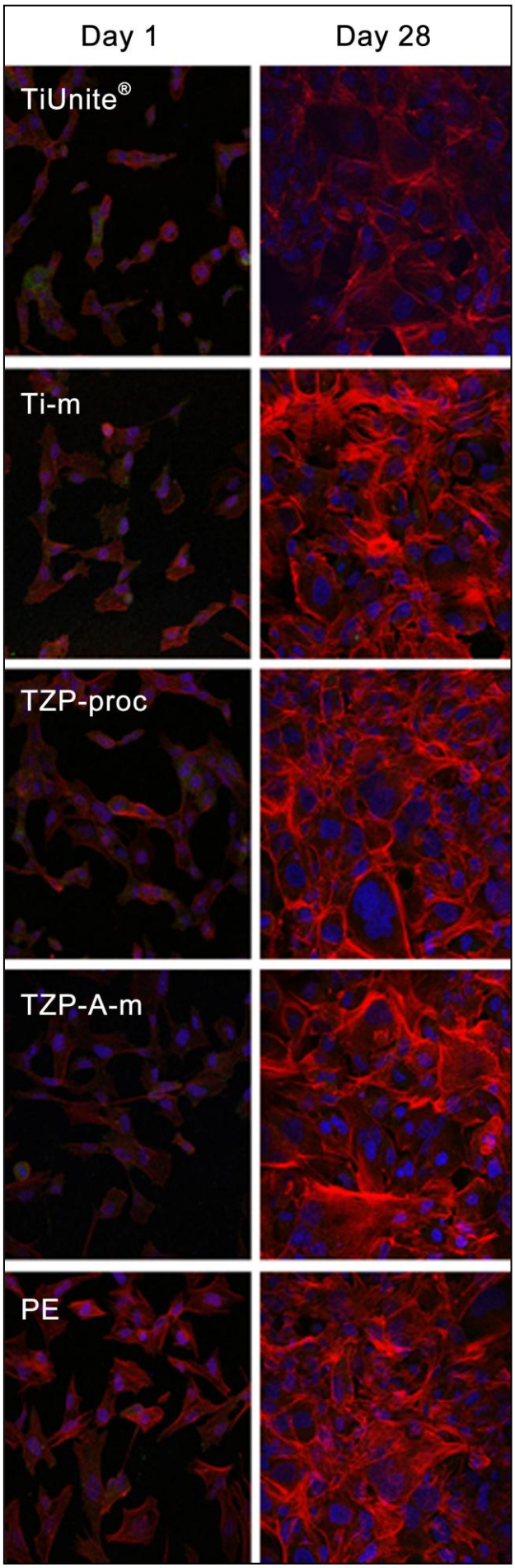

Fig. 4. The cytoskeletal arrangement of the osteoblasts was examined by indirect immunofluorescence of the focal adhesion protein vinculin and the cytoskeleton protein actin. To visualize the evolution of the cytoskeleton and focal adhesions of hFOB 1.19 after culturing 1 and 28 days on the different surfaces, actin and vinculin immunostaining was used (actin = red; nucleoli = blue; vinculin = green).

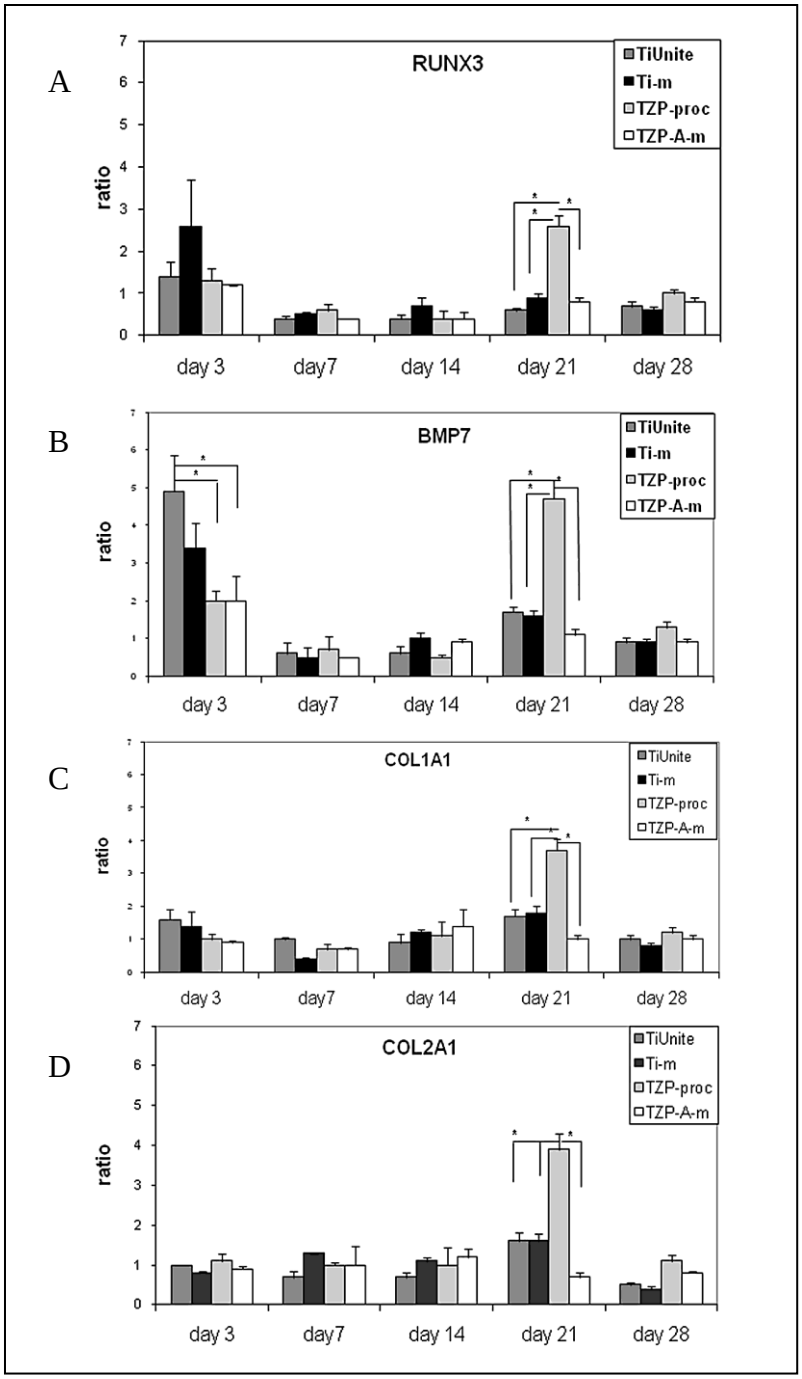

Fig. 5. (A) RUNX3 was upregulated on Ti-m at day 3 and on the TZP-proc surface at day 21. (B) BMP7 was upregulated at day 3 on TiUnite. There was a noticeable upregulation on the TZP-proc surface and a downregulation on the titanium surfaces at day 21. (C) COL1A1 seemed to be only little regulated except for day 21 when a significant upregulation occurred on the TZP-proc surface. (D) COL2A1, like COL1A1, encodes for osteoblast matrix proteins. Only at day 21, a significant upregulation occurred on the TZP-proc surface.

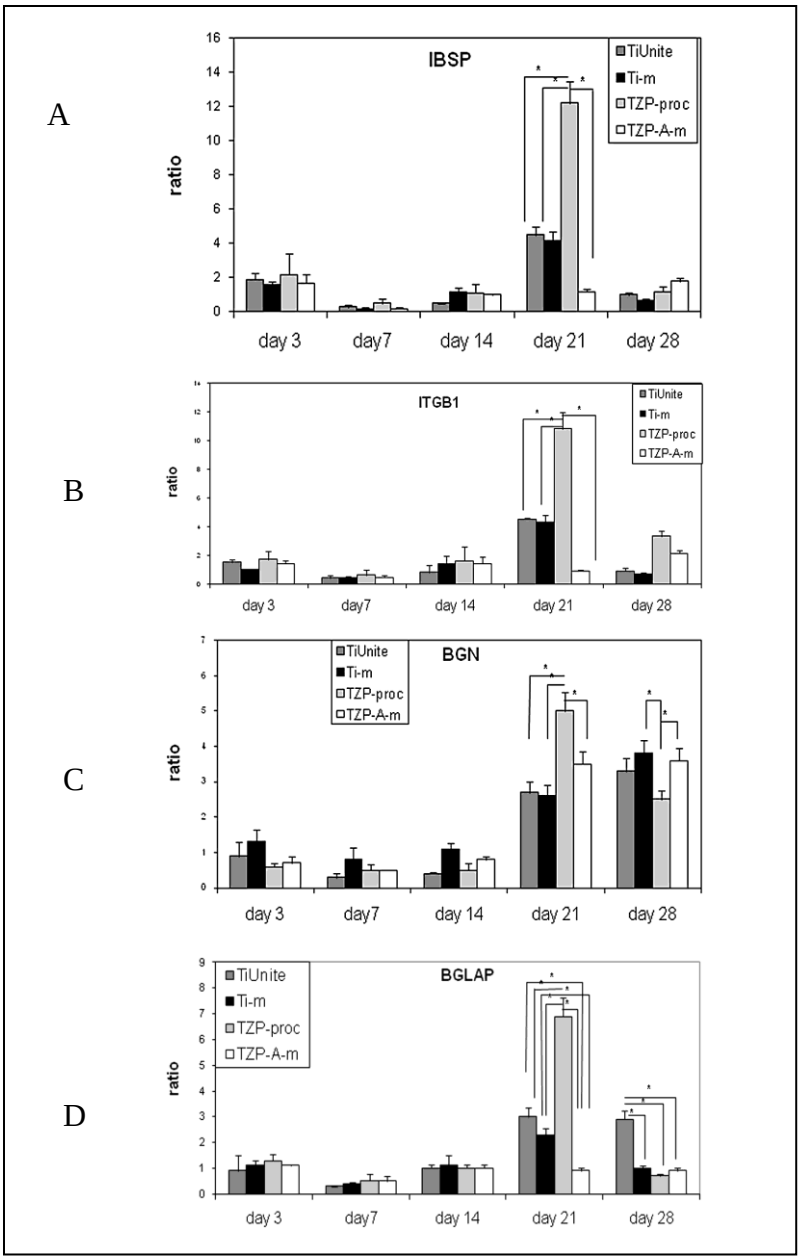

Fig. 6. (A) IBSP was not upregulated until day 21. The upregulation of IBSP was significant on the TZP-proc substrate. (B) Like for IBSP, TZP-proc induced a significant upregulation of ITGB1 on day 21. (C) BGN - as an essential component of the ECM - was upregulated at day 21. This upregulation occurred significantly more on the TZP-proc surface compared to all other surfaces. At day 28, a downregulation of BGN on TZP-proc could be seen. The BGN gene expression on the other surfaces remained at similar levels as on day 21. (D) Osteocalcin (BGLAP) - a bone specific marker for matrix mineralization – was upregulated on TZP-proc at day 21. At day 28, a significant downregulation was observed on the TZP-proc surface.

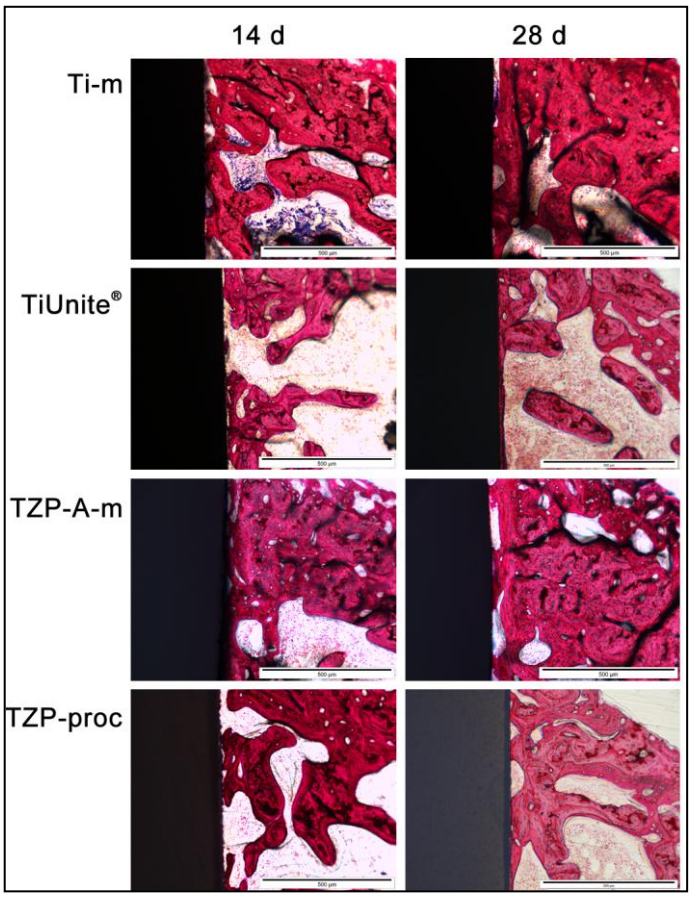

Fig. 7. At day 14 and day 21, the histological pictures showed direct mineralized bone-to implant contacts at all zirconia and titanium implant surfaces. The mineralized bone-to-implant contact was interrupted by bone marrow-to-implant contact.

9 References

1. Denry I and Kelly J R. State of the art of zirconia for dental applications. Dent Mater, 2008; 24:299-307.

2. Holst S, Blatz M B, Hegenbarth E, Wichmann M and Eitner S. Prosthodontic considerations for predictable single-implant esthetics in the anterior maxilla. J Oral Maxillofac Surg, 2005; 63:89-96.

3. Levin L, Pathael S, Dolev E and Schwartz-Arad D. Aesthetic versus surgical success of single dental implants: 1- to 9-year follow-up. Pract Proced Aesthet Dent, 2005; 17:533-538.

4. Sailer I, Philipp A, Zembic A, Pjetursson B E, Hämmerle C H and Zwahlen M. A systematic review of the performance of ceramic and metal implant abutments supporting fixed implant reconstructions. Clin Oral Implants Res, 2009; 20 Suppl 4:4-31.

5. Weingart D, Steinemann S, Schilli W, Strub J R, Hellerich U, Assenmacher J and Simpson J. Titanium deposition in regional lymph nodes after insertion of titanium screw implants in maxillofacial region. Int J Oral Maxillofac Surg, 1994; 23:450-452.

6. Bianco P D, Ducheyne P and Cuckler J M. Local accumulation of titanium released from a titanium implant in the absence of wear. J Biomed Mater Res 1996; 31:227-234.

7. Egusa H, Ko N, Shimazu T and Yatani H. Suspected association of an allergic reaction with titanium dental implants: A clinical report. J Prosthet Dent, 2008; 100:344-347.

8. Sicilia A, Cuesta S, Coma G, Arregui I, Guisasola C, Ruiz E and Maestro A. Titanium allergy in dental implant patients: A clinical study on 1500 consecutive patients. Clin Oral Implants Res, 2008; 19:823-835.

9. Adell R, Lekholm U, Rockler B and Brånemark P I. A 15-year study of osseointegrated implants in the treatment of the edentulous jaw. Int J Oral Surg, 1981; 10:387-416.

10. Adell R, Eriksson B, Lekholm U, Brånemark P I and Jemt T. Long-term follow-up study of osseointegrated implants in the treatment of totally edentulous jaws. Int J Oral Maxillofac Implants, 1990; 5:347-359.

11. van Steenberghe D. A retrospective multicenter evaluation of the survival rate of osseointegrated fixtures supporting fixed partial prostheses in the treatment of partial edentulism. J Prosthet Dent, 1989; 61:217-223.

12. Jemt T. Modified single and short-span restorations supported by osseointegrated fixtures in the partially edentulous jaw. J Prosthet Dent, 1986; 55:243-247.

13. Esposito M, Murray-Curtis L, Grusovin M G, Coulthard P and Worthington H V. Interventions for replacing missing teeth: Different types of dental implants. Cochrane Database Syst Rev, 2007; CD003815.

14. Chevalier J. What future for zirconia as a biomaterial? Biomaterials, 2006; 27:535-543.

15. Andreiotelli M, Wenz H J and Kohal R J. Are ceramic implants a viable alternative to titanium implants? A systematic literature review. Clin Oral Implants Res, 2009; 20 Suppl 4:32-47.

16. Andreiotelli M and Kohal R J. Fracture strength of zirconia implants after artificial aging. Clin Implant Dent Relat Res, 2009; 11:158-166.

17. Kohal R J, Klaus G and Strub J R. Zirconia-implant-supported all-ceramic crowns withstand long-term load: A pilot investigation. Clin Oral Implants Res, 2006; 17:565-571.

18. Silva N R, Coelho P G, Fernandes C A, Navarro J M, Dias R A and Thompson V P. Reliability of one-piece ceramic implant. J Biomed Mater Res B Appl Biomater, 2009; 88:419-426.

19. Kohal R J, Wolkewitz M and Mueller C. Alumina-reinforced zirconia implants: Survival rate and fracture strength in a masticatory simulation trial. Clin Oral Implants Res, 2010; 21:1345-1352.

20. Akagawa Y, Hosokawa R, Sato Y and Kamayama K. Comparison between freestanding and tooth-connected partially stabilized zirconia implants after two years' function in monkeys: A clinical and histologic study. J Prosthet Dent, 1998; 80:551-558.

21. Scarano A, Di Carlo F, Quaranta M and Piattelli A. Bone response to zirconia ceramic implants: An experimental study in rabbits. J Oral Implantol, 2003; 29:8-12.

22. Kohal R J, Weng D, Bächle M and Strub J R. Loaded custom-made zirconia and titanium implants show similar osseointegration: An animal experiment. J Periodontol, 2004; 75:1262-1268.

23. Kohal R J, Wolkewitz M, Hinze M, Han J S, Bächle M and Butz F. Biomechanical and histological behavior of zirconia implants: An experiment in the rat. Clin Oral Implants Res, 2009; 20:333-339.

24. Lee J, Sieweke J H, Rodriguez N A, Schüpbach P, Lindström H, Susin C and Wikesjö U M. Evaluation of nano-technology-modified zirconia oral implants: A study in rabbits. J Clin Periodontol, 2009; 36:610-617.

25. Rocchietta I, Fontana F, Addis A, Schupbach P and Simion M. Surface-modified zirconia implants: Tissue response in rabbits. Clin Oral Implants Res, 2009; 20:844-850.

26. Brånemark P I, Hansson B O, Adell R, Breine U, Lindström J, Hallén O and Ohman A. Osseointegrated implants in the treatment of the edentulous jaw. Experience from a 10-year period. Scand J Plastic Reconstr Surg, 1977; Supplementum 16:1-132.

27. Klokkevold P R, Nishimura R D, Adachi M and Caputo A. Osseointegration enhanced by chemical etching of the titanium surface. A torque removal study in the rabbit. Clin Oral Implants Res, 1997; 8:442-447.

28. Baker D, London R M and O'Neal R. Rate of pull-out strength gain of dual-etched titanium implants: A comparative study in rabbits. Int J Oral Maxillofac Implants, 1999; 14:722-728.

29. Ogawa T, Ozawa S, Shih J H, Ryu K H, Sukotjo C, Yang J M and Nishimura I. Biomechanical evaluation of osseous implants having different surface topographies in rats. J Dent Res, 2000; 79:1857-1863.

30. Butz F, Aita H, Wang C J and Ogawa T. Harder and stiffer bone osseointegrated to roughened titanium. J Dent Res, 2006; 85:560-565.

31. Galli C, Guizzardi S, Passeri G, Martini D, Tinti A, Mauro G and Macaluso G M. Comparison of human mandibular osteoblasts grown on two commercially available titanium implant surfaces. J Periodontol, 2005; 76:364-372.

32. Bowers K T, Keller J C, Randolph B A, Wick D G and Michaels C M. Optimization of surface micromorphology for enhanced osteoblast responses in vitro. Int J Oral Maxillofac Implants, 1992; 7:302-310.

33. Brunette D M. The effects of implant surface topography on the behavior of cells. Int J Oral Maxillofac Implants, 1988; 3:231-246.

34. Groessner-Schreiber B and Tuan R S. Enhanced extracellular matrix production and mineralization by osteoblasts cultured on titanium surfaces in vitro. Journal of Cell Science, 1992; 101:209-217.

35. Ong J L, Prince C W, Raikar G N and Lucas L C. Effect of surface topography of titanium on surface chemistry and cellular response. Implant Dent, 1996; 5:83-88.

36. Zreiqat H and Howlett C R. Titanium substrata composition influences osteoblastic phenotype: In vitro study. J Biomed Mater Res 1999; 47:360-366.

37. Isa Z M, Schneider G B, Zaharias R, Seabold D and Stanford C M. Effects of fluoride-modified titanium surfaces on osteoblast proliferation and gene expression. Int J Oral Maxillofac Implants, 2006; 21:203-211.

38. Ferguson S J, Langhoff J D, Voelter K, von Rechenberg B, Scharnweber D, Bierbaum S, Schnabelrauch M, Kautz A R, Frauchiger V M, Mueller T L, van Lenthe G H and Schlottig F. Biomechanical comparison of different surface modifications for dental implants. Int J Oral Maxillofac Implants, 2008; 23:1037-1046.

39. Bacchelli B, Giavaresi G, Franchi M, Martini D, De Pasquale V, Trire A, Fini M, Giardino R and Ruggeri A. Influence of a zirconia sandblasting treated surface on peri-implant bone healing: An experimental study in sheep. Acta Biomater, 2009; 5:2246-2257.

40. Lee J, Sieweke J H, Rodriguez N A, Schupbach P, Lindstrom H, Susin C and Wikesjo U M. Evaluation of nano-technology-modified zirconia oral implants: A study in rabbits. J Clin Periodontol, 2009; 36:610-617.

41. Sennerby L, Dasmah A, Larsson B and Iverhed M. Bone tissue responses to surface-modified zirconia implants: A histomorphometric and removal torque study in the rabbit. Clin Implant Dent Relat Res, 2005; 7 Suppl 1:S13-20.

42. Hoffmann O, Angelov N, Zafiropoulos G G and Andreana S. Osseointegration of zirconia implants with different surface characteristics: An evaluation in rabbits. Int J Oral Maxillofac Implants, 27:352-358.

43. Subramaniam M, Jalal S M, Rickard D J, Harris S A, Bolander M E and Spelsberg T C. Further characterization of human fetal osteoblastic hfob 1.19 and hfob/er alpha cells: Bone formation in vivo and karyotype analysis using multicolor fluorescent in situ hybridization. J Cell Biochem, 2002; 87:9-15.

44. Pfaffl M W. A new mathematical model for relative quantification in real-time rt-pcr. Nucleic Acids Research, 2001; 29:e45.

45. Donath K and Breuner G. A method for the study of undecalcified bones and teeth with attached soft tissues. The sage-schliff (sawing and grinding) technique. J Oral Pathol, 1982; 11:318-326.

46. Ozawa S, Ogawa T, Iida K, Sukotjo C, Hasegawa H, Nishimura R D and Nishimura I. Ovariectomy hinders the early stage of bone-implant integration: Histomorphometric, biomechanical, and molecular analyses. Bone, 2002; 30:137-143.

47. Levanon D, Negreanu V, Bernstein Y, Bar-Am I, Avivi L and Groner Y. Aml1, aml2, and aml3, the human members of the runt domain gene-family: Cdna structure, expression, and chromosomal localization. Genomics, 1994; 23:425-432.

48. Komori T. Regulation of osteoblast differentiation by transcription factors. J Cell Biochem, 2006; 99:1233-1239.

49. Mizuno M, Fujisawa R and Kuboki Y. Bone chondroadherin promotes attachment of osteoblastic cells to solid-state substrates and shows affinity to collagen. Calcif Tissue Int, 1996; 59:163-167.

50. Imai S, Kaksonen M, Raulo E, Kinnunen T, Fages C, Meng X, Lakso M and Rauvala H. Osteoblast recruitment and bone formation enhanced by cell matrix-associated heparin-binding growth-associated molecule (hb-gam). J Cell Biol, 1998; 143:1113-1128.

51. Davies J E. Mechanisms of endosseous integration. Int J Prosthodont, 1998; 11:391-401.

52. Verrier S, Peroglio M, Voisard C, Lechmann B and Alini M. The osteogenic differentiation of human osteoprogenitor cells on anodic-plasma-chemical treated ti6al7nb. Biomaterials, 2011; 32:672-680.

53. Meredith D O, Eschbach L, Riehle M O, Curtis A S and Richards R G. Microtopography of metal surfaces influence fibroblast growth by modifying cell shape, cytoskeleton, and adhesion. J Orthop Res, 2007; 25:1523-1533.

54. Silva T S, Machado D C, Viezzer C, Silva Junior A N and de Oliveira M G. Effect of titanium surface roughness on human bone marrow cell proliferation and differentiation: An experimental study. Acta Cir Bras, 2009; 24:200-205.

55. Kunzler T P, Drobek T, Schuler M and Spencer N D. Systematic study of osteoblast and fibroblast response to roughness by means of surface-morphology gradients. Biomaterials, 2007; 28:2175-2182.

56. Setzer B, Bächle M, Metzger M C and Kohal R J. The gene-expression and phenotypic response of hfob 1.19 osteoblasts to surface-modified titanium and zirconia. Biomaterials, 2009; 30:979-990.

57. Moursi A M, Damsky C H, Lull J, Zimmerman D, Doty S B, Aota S and Globus R K. Fibronectin regulates calvarial osteoblast differentiation. Journal of Cell Science, 1996; 109:1369-1380.

58. Garcia A J and Boettiger D. Integrin-fibronectin interactions at the cell-material interface: Initial integrin binding and signaling. Biomaterials, 1999; 20:2427-2433.

59. Schwartz M A, Schaller M D and Ginsberg M H. Integrins: Emerging paradigms of signal transduction. Annual Review of Cell and Developmental Biology, 1995; 11:549-599.

60. Howe A, Aplin A E, Alahari S K and Juliano R L. Integrin signaling and cell growth control. Current Opinion in Cell Biology, 1998; 10:220-231.

61. Ogawa T and Nishimura I. Different bone integration profiles of turned and acid-etched implants associated with modulated expression of extracellular matrix genes. Int J Oral Maxillofac Implants, 2003; 18:200-210.

62. Helfrich M H, Nesbitt S A, Lakkakorpi P T, Barnes M J, Bodary S C, Shankar G, Mason W T, Mendrick D L, Vaananen H K and Horton M A. Beta 1 integrins and osteoclast function: Involvement in collagen recognition and bone resorption. Bone, 1996; 19:317-328.

63. McCracken M, Lemons J E and Zinn K. Analysis of ti-6al-4v implants placed with fibroblast growth factor 1 in rat tibiae. Int J Oral Maxillofac Implants, 2001; 16:495-502.

64. Howlett C R. Early bone formation around calcium-ion-implanted titanium inserted into rat tibia. J Biomed Mater Res 1999; 44:352-353.

65. Brånemark R, Ohrnell L O, Nilsson P and Thomsen P. Biomechanical characterization of osseointegration during healing: An experimental in vivo study in the rat. Biomaterials, 1997; 18:969-978.

66. Abron A, Hopfensperger M, Thompson J and Cooper L F. Evaluation of a predictive model for implant surface topography effects on early osseointegration in the rat tibia model. J Prosthet Dent, 2001; 85:40-46.

67. Deligianni D D, Katsala N, Ladas S, Sotiropoulou D, Amedee J and Missirlis Y F. Effect of surface roughness of the titanium alloy ti-6al-4v on human bone marrow cell response and on protein adsorption. Biomaterials, 2001; 22:1241-1251.

68. Wennerberg A, Albrektsson T and Andersson B. Bone tissue response to commercially pure titanium implants blasted with fine and coarse particles of aluminum oxide. Int J Oral Maxillofac Implants, 1996; 11:38-45.

69. Gotfredsen K, Berglundh T and Lindhe J. Anchorage of titanium implants with different surface characteristics: An experimental study in rabbits. Clin Implant Dent Relat Res, 2000; 2:120-128.

70. Cochran D L, Nummikoski P V, Higginbottom F L, Hermann J S, Makins S R and Buser D. Evaluation of an endosseous titanium implant with a sandblasted and acid-etched surface in the canine mandible: Radiographic results. Clin Oral Implants Res, 1996; 7:240-252.

71. Turner C H and Burr D B. Basic biomechanical measurements of bone: A tutorial. Bone, 1993; 14:595-608.

72. Garetto L P, Chen J, Parr J A and Roberts W E. Remodeling dynamics of bone supporting rigidly fixed titanium implants: A histomorphometric comparison in four species including humans. Implant Dent, 1995; 4:235-243.

73. Suzuki K, Aoki K and Ohya K. Effects of surface roughness of titanium implants on bone remodeling activity of femur in rabbits. Bone, 1997; 21:507-514.

74. Wennerberg A and Albrektsson T. Effects of titanium surface topography on bone integration: A systematic review. Clin Oral Implants Res, 2009; 20 Suppl 4:172-184.

75. Gahlert M, Röhling S, Wieland M, Sprecher C M, Kniha H and Milz S. Osseointegration of zirconia and titanium dental implants: A histological and histomorphometrical study in the maxilla of pigs. Clin Oral Implants Res, 2009; 20:1247-1253.

76. Koch F P, Weng D, Kramer S, Biesterfeld S, Jahn-Eimermacher A and Wagner W. Osseointegration of one-piece zirconia implants compared with a titanium implant of identical design: A histomorphometric study in the dog. Clin Oral Implants Res, 2010; 21:350-356.